

# Surface subsidence characteristics of grout injection into overburden: case study of Yuandian No. 2 coalmine, China

Hao Teng<sup>1,2</sup> · Jialin Xu<sup>1,2</sup> · Dayang Xuan<sup>2</sup> · Binglong Wang<sup>1,2</sup>

Received: 29 June 2015 / Accepted: 15 December 2015 / Published online: 19 March 2016  
© Springer-Verlag Berlin Heidelberg 2016

**Abstract** A study on the surface subsidence characteristics is essential for evaluating the effects of subsidence control technologies and improving such technologies. One such technology is grout injection into overburden (GIO), which is used in coal mining areas. In the past, the subsidence reduction ratio—a single index—was often used to evaluate the final amount of subsidence control achieved by GIO; however, little research has been conducted on the dynamic process of surface subsidence. In this study, the surface subsidence characteristics of GIO on the side of a stopping line (SSL) of a longwall were examined through in situ monitoring, and the characteristics of areas with grouting were compared with those without. The final maximum subsidence, horizontal displacement, and subsidence rate decreased considerably (70.2, 80.4, and 77.5 %, respectively) with the use of GIO. However, 4.6 % of the mining height subsided at a certain surface point on the SSL before GIO controlled subsidence at that point. Compared with the duration of the active period without grouting, that with grouting and the corresponding subsidence decreased considerably (44.2 and 87.1 %, respectively). Generally, it is quite difficult to control the surface subsidence when GIO is implemented on the SSL of a longwall because the surface and subsurface are already affected by the coal extraction, without grouting on the side of the open-off cut. Thus, the success of GIO technology in

the case study described in this paper demonstrates its effectiveness in controlling the surface subsidence in coal mining areas.

**Keywords** Surface subsidence · Subsidence control · Grout injection into overburden · Bedding plane separation

## Introduction

Surface subsidence is a frequent geological disaster (Singh 2007; Wu et al. 2009a; Choi et al. 2010) that causes environmental and social problems, such as damage to farmlands and civic structures as well as waterlogging in the affected area (Wu et al. 2009b; Can et al. 2012, 2013; Dong et al. 2015). Therefore, developing effective technologies for controlling the surface subsidence has been the focus of researchers over the past few decades. Artificial recharge and goaf backfilling technologies are often used to control surface subsidence caused by underground water extraction (de los Cobos 2015) and coal mining (Lokhande et al. 2005; Junker and Witthaus 2013; Witthaus et al. 2013; Xuan et al. 2013; Zhang et al. 2015), respectively. However, irrespective of the technology employed, studies on the corresponding surface subsidence characteristics are common and are of interest, as they are important for evaluating the effectiveness and applicability of the technology, as well as ultimately improving it.

Grout injection into overburden (GIO) is a surface subsidence control technology that is applied in coal mining areas, wherein fly ash slurry is injected into bedding plane separations by pumping through surface boreholes when the longwall face advances to support the overburden, thus controlling the surface subsidence (Chen and Guo 2008; Xuan and Xu 2014). The use of this

✉ Jialin Xu  
cumtxjl@cumt.edu.cn

<sup>1</sup> School of Mines, China University of Mining and Technology, Xuzhou 221116, Jiangsu, China

<sup>2</sup> State Key Laboratory of Coal Resources and Safe Mining, China University of Mining and Technology, Xuzhou 221116, Jiangsu, China

technology has increased in recent years (Palarski 1989; Guo et al. 2007; Xuan et al. 2014; Xuan and Xu 2014). However, an approach for evaluating its effectiveness has not yet been determined, and this is a key problem that remains to be solved. The effectiveness of GIO depends on the final subsidence value and the dynamic characteristics of the surface subsidence. To this end, considerable research has been conducted. The subsidence reduction ratio—which is defined as the ratio of the difference between the surface subsidence without and with grouting to the surface subsidence without grouting—is used to evaluate the final amount of subsidence control achieved (Chen and Guo 2008; Xuan and Xu 2014). Additionally, surface deformation parameters (inclination, curvature, and horizontal strain) are often used to evaluate the degree of damage caused to buildings owing to surface subsidence. These abovementioned studies have considerably helped in the evaluation of the final amount of subsidence control achieved by GIO, but they have not considered the dynamic characteristics of surface subsidence, such as the subsidence rate, advance subsidence (refer to “[Advance subsidence](#)”), and the duration of surface subsidence. Since actual surface subsidence is dynamic in nature, a study of the dynamic parameters would be essential for evaluating the influence of surface subsidence on buildings. Traditionally, the subsidence reduction ratio has often been calculated based on the predicted maximum surface subsidence without grouting; these predicted values sometimes show a large deviation from the actual values. Thus, field monitoring is required to confirm the final amount of subsidence control achieved by GIO.

This study was conducted to examine the surface subsidence characteristics of GIO through in situ monitoring and to assess the differences between the dynamic characteristics of surface subsidence with grouting and that without grouting. The research results are used to further verify the final amount of subsidence control achieved by GIO.

## Site description

The Yuandian No. 2 coalmine, operated by the Huaibei Mining Group Co., Ltd., is located in Anhui Province, China. This coalmine has always been an area of conflict owing to the damage caused to the ground buildings during coal extraction. Longwall 7226, the focus of this study, is a typical case, and there is an area spanning 316 m on the side of the stopping line (SSL) of Longwall 7226; this area is affected by a village (Fig. 1). The village, which covers an area of 0.94 km<sup>2</sup>, has 1600 households and 8000 residents. Most of the buildings are two-story or three-story brick–concrete structures (Fig. 1). It would cost 450

million Yuan—a fee that the mine cannot afford—to relocate the village to extract coal in the affected area. Furthermore, it would take a long time to relocate the village, impacting regular operation to a great extent. Except for the village, the farmland is located on the ground surface shown in Fig. 1. The area that was affected by the extraction of 544 m of Longwall 7226 on the side of the open-off cut (SOC) was not under conservation, and the reclamation of this area, as specified by the Chinese government, would be carried out after mining operations are complete.

GIO was implemented to protect the ground buildings when 316 m of Longwall 7226 on the SSL in the strike direction was extracted, whereas 544 m of this longwall on the SOC in the strike direction was mined with full caving (i.e., without grouting). However, it is difficult to implement GIO on the SSL of a longwall, such as Longwall 7226. When GIO is implemented on the SSL of a longwall, the SOC is already extracted without grouting (i.e., with full subsidence in the strike direction), which disturbs the surface and subsurface of the SSL. Nevertheless, this unique condition is favorable for studying the surface subsidence characteristics of GIO and for comparison with the surface subsidence characteristics obtained without grouting.

## Geological and mining conditions

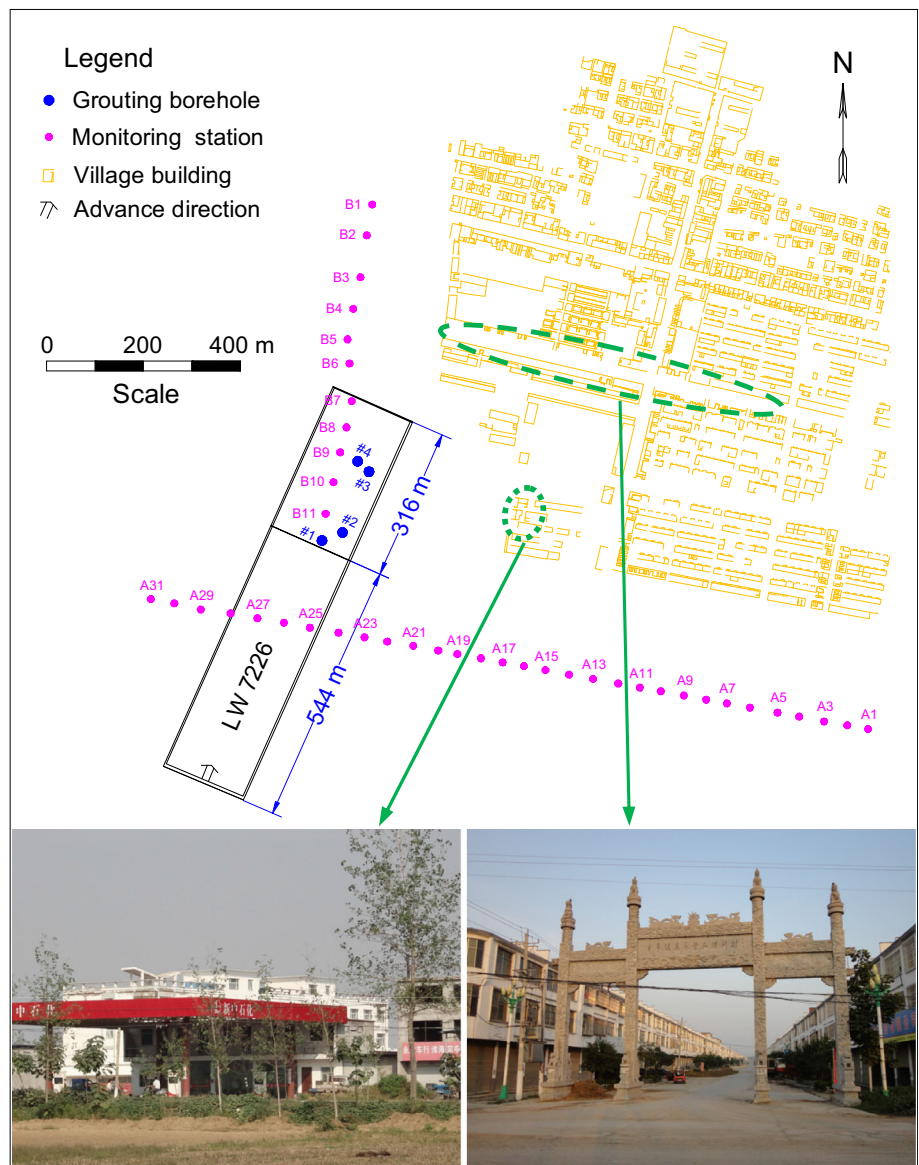
The Yuandian No. 2 coalmine is located in the Huanghuai plain. The landscape in this area is flat, with an average elevation of 28 m above sea level. The strata sequence from bottom to top is as follows: the Shanxi Formation (Lower Permian) (P1s), with a thickness of 103 m; the Xiashihezi Formation (Lower Permian) (P1x), with a thickness of 261 m; the Neogene System (N), with a thickness of 171 m; and the Quaternary System (Q), with a thickness of 87 m. The P1s and P1x formations are mainly composed of fine sandstone, siltstone, mudstone, and coal, while the N and Q systems are mainly composed of clay, sand, and gravel.

Longwall 7226, which has an inclined width of 180 m and a strike length of 860 m, is the first panel of Mining Section 82. The extracted coal seam is Seam No. 72, which has an average thickness of 5.0 m. It is in the P1x formation and at an average angle of 4°. Within the study area, this coal seam is overlain by 444–489 m of overburden, which includes approximately 260 m of alluvium. A borehole log for the study site is shown in Fig. 2.

## GIO field trial

To protect the ground buildings, four surface boreholes with diameters of 156 mm (#1–4; Fig. 1) were used to

**Fig. 1** Plan view showing surface and underground features of the study site and photographs of structures on the site



implement GIO during the extraction of the SSL of Longwall 7226. Details of the locations of the boreholes are given in Table 1. Fly ash produced by a power plant was selected as the grouting material. Fly ash was stored in a fly ash tank, and then conveyed to a mixing tank through a screw feeder. At the same time, water was conveyed to the mixing tank. The slurry formed by mixing water and fly ash in the ratio 1.6:1.0–2.0:1.0 was then conveyed to a second mixing tank. After mixing again, the slurry was pumped by grouting pumps into bedding plane separations through the surface boreholes (Fig. 3).

The extraction of the SOC began on January 20, 2013. The extraction of the SSL and the implementation of GIO began on August 4, 2013, and ended on December 11, 2013. The total grouting volume reached 107,256 tons.

## Methodology and results

### Methodology

Surface monitoring stations were established to study the surface subsidence characteristics of GIO and compare

Columnar	Lithology	Thickness (m)	Cover depth (m)
	Alluvium	257.80	257.80
	Mudstone	42.89	300.69
	Fine sandstone	11.44	312.13
	Mudstone	18.00	330.13
	Coal seam	0.55	330.68
	Mudstone	0.92	331.60
	Coal seam	0.72	332.32
	Mudstone	4.05	336.37
	Siltstone	9.30	345.67
	Mudstone	3.09	348.76
	Coal seam	0.42	349.18
	Siltstone	10.55	359.73
	Fine sandstone	2.66	362.39
	Siltstone	2.95	365.34
	Mudstone	14.03	379.37
	Siltstone	12.92	392.29
	Fine sandstone	3.67	395.96
	Siltstone	4.04	400.00
	Fine sandstone	2.66	402.66
	Mudstone	2.30	404.96
	Coal seam #5 <sub>1</sub>	0.46	405.42
	Mudstone	10.37	415.79
	Coal seam	0.27	416.06
	Mudstone	8.83	424.89
	Siltstone	10.22	435.11
	Mudstone	1.88	436.99
	Fine sandstone	2.69	439.68
	Mudstone	13.44	453.12
	Coal seam	0.51	453.63
	Mudstone	4.28	457.91
	Fine sandstone	2.38	460.29
	Coal seam #6 <sub>3</sub>	0.53	460.82
	Mudstone	1.75	462.57
	Coal seam	0.41	462.98
	Mudstone	4.35	467.33
	Siltstone	3.15	470.48
	Fine sandstone	12.16	482.64
	Mudstone	1.47	484.11
	Coal seam #7 <sub>2</sub>	4.62	488.73

Fig. 2 Borehole log for the study site (not to scale)

Table 1 Locations of the grouting boreholes for Longwall 7226 (m)

	#1	#2	#3	#4
Distance to the open-off cut	561	593	731	736
Distance to the stopping line	299	267	129	124
Distance to the head gate	109	141	140	110
Distance to the tail gate	71	39	40	70

them with the surface subsidence characteristics without grouting. The monitoring stations consisted of two measurement lines: along the strike (line B) and along the inclination (line A) of Longwall 7226 (Fig. 1). In addition, there were 11 monitoring stations (i.e., B1–B11, from north to south) along the strike line and 31 monitoring stations (i.e., A1–A31, from east to west) along the inclination line. The surface subsidence was monitored from March 21, 2013 to November 16, 2014 using an electronic digital level. The model of the electronic digital level is Leica

DNA03, which has a 0.3 mm standard deviation per km double leveling (invar staff) for height measurement. During this period, Line A and Line B were observed 35 and 33 times, respectively. The horizontal displacement was measured via a total station on November 16, 2014. The model of the total station is Leica TS06, which has a measurement accuracy of 2'' for angle measurement and 1.5 mm + 2.0 ppm for range measurement. Unfortunately, Stations A26 and A28 failed before the final round of monitoring. The subsidence of these two stations as of November 16, 2014 was calculated via interpolation and checked using values obtained in the second-to-last monitoring cycle. During the extraction, the positions of the working face were recorded every day.

Results

The root mean square error values of the vertical displacements range from 0.8 to 2.5 mm for 35 measurement iterations (from March 21, 2013 to November 16, 2014), while the root mean square error values of the horizontal displacements range from 1.6 to 7.4 mm for the measurements conducted on November 16, 2014. The final vertical displacement and horizontal displacement vectors of the monitoring stations are shown in Figs. 4 and 5, respectively. Without grouting, the maximal vertical displacement and horizontal displacement on the SOC of Longwall 7226 were 2509.2 mm (Station A27) and 960.3 mm (Station A25), respectively. By comparison, the vertical displacement and horizontal displacement of Station B10, located near the center of the grout-injected area were 748.5 and 169.0 mm, respectively. Therefore, the subsidence reduction ratio and the reduction ratio of the maximum horizontal displacement were 70.2 and 82.4 %, respectively.

Inclination, curvature, and horizontal strain are three primary indicators used to characterize the surface deformations. The difference in surface subsidence between two adjacent points of a line section in the subsidence basin divided by the horizontal distance between the two points is referred to as the inclination of the section. The difference in inclination between two adjacent sections divided by the average length of the two sections is referred to as the curvature. Positive values indicate bulges at the surface, whereas negative values represent depressions at the surface. The difference in horizontal displacement between two adjacent points divided by the distance between those two points is referred to as the horizontal strain. Positive horizontal strains indicate tensile deformation, whereas negative values indicate compressive deformation. Based

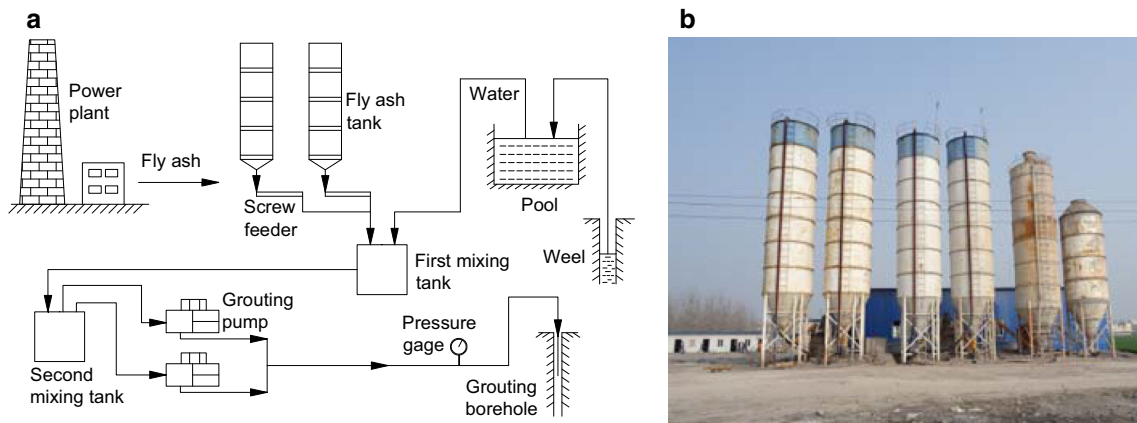


**Fig. 3** Grouting system. **a** Schematic diagram (Xuan and Xu 2014). **b** Photograph of grouting station

on the monitoring results of vertical and horizontal displacements, the deformations in both the areas with grouting and those without grouting were calculated (Fig. 6). The maximum values are listed in Table 2.

The final deformation values indicate that the damage in the area without grouting reached Level IV with respect to the classification of damage to surface brick–concrete structures (Table 3) by the Chinese State Bureau of Coal Industry (2000). The damage in the area with grouting was controlled within Level I, and no visible cracks appeared on the walls of the buildings, which imply that no repairs were required. In other words, the buildings were protected well by the implementation of GIO and remained available for normal use.

**Dynamic characteristics of surface subsidence of GIO**

This section discusses three dynamic parameters of surface subsidence: the maximum subsidence rate, advance subsidence, and the duration of surface subsidence of GIO. Values of these parameters with and without grouting are compared.

**Maximum subsidence rate**

The subsidence rate is the most visible dynamic parameter reflecting the degree of surface damage that occurs during the surface subsidence. According to the results, the maximum subsidence rate was up to 26.83 mm/day on the SOC of Longwall 7226; whereas the rate during GIO on the SSL was 6.03 mm/day (refer to Fig. 8 in “Duration of surface subsidence”). The reduction ratio of the maximum subsidence

rate was 77.5 %, which demonstrates that GIO clearly helps control the dynamic process of surface subsidence.

**Advance subsidence**

In this study, the parameter of advance subsidence, which reflects the dynamic surface subsidence, is proposed. Advance subsidence is defined as the subsidence of the surface directly above the working face as it advances. Since the grout generally diffuses to the overburden directly above a working face or around it as a longwall advances (Xuan et al. 2015), advance subsidence at a certain surface point under GIO is regarded as the subsidence that occurs before GIO controls subsidence at that point. It can be inferred that when the mining height is greater, advance subsidence will increase, which implies that ground buildings may not be protected adequately. Thus, it is necessary to evaluate the ratio of advance subsidence to the mining height.

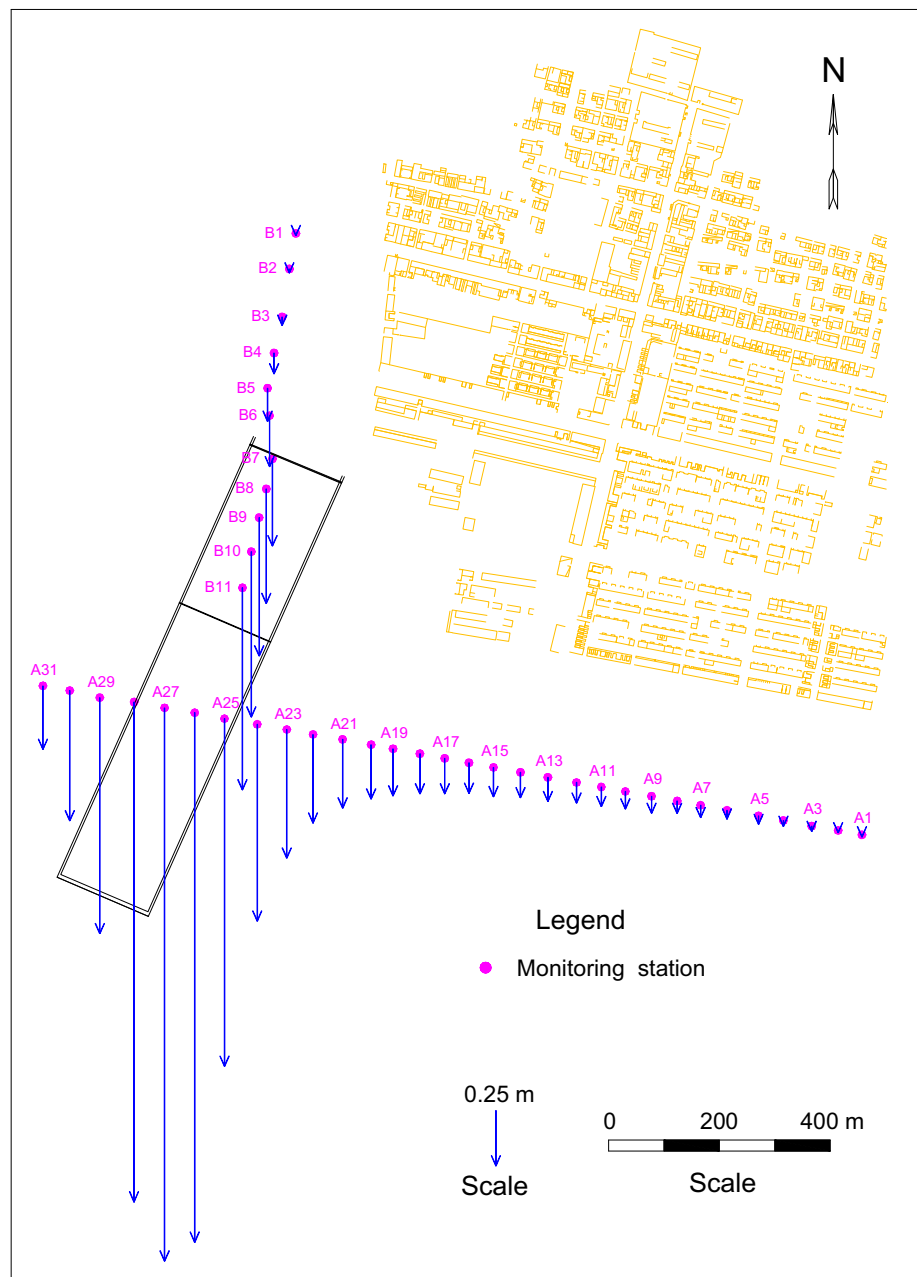
In this study, advance subsidence without grouting was 684.0 mm on the SOC of Longwall 7226, and that with grouting on the SSL was 228.0 mm (Fig. 7). The reduction ratio was up to 66.7 %, which indicates substantial control of surface subsidence. The results also show that 4.6 % of the mining height subsided at a certain surface point on the SSL before GIO controlled subsidence at the point.

**Duration of surface subsidence**

The duration of surface subsidence, which is often calculated from the subsidence rate, is the time from which a station begins to move till the end of subsidence. The duration of surface subsidence after implementing GIO is expected to differ from that without implementing



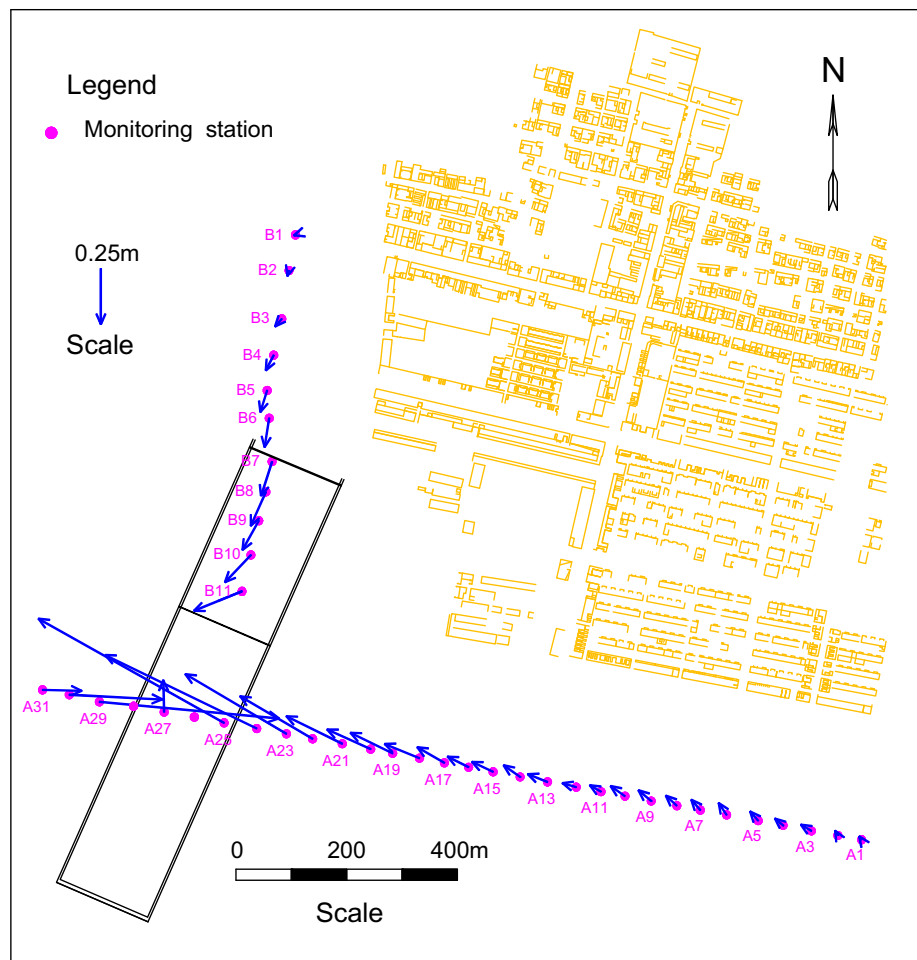
**Fig. 4** Final vertical displacement vectors of the monitoring stations



grouting. In traditional longwall mining (without grouting), the duration of surface subsidence can be divided into three periods according to the subsidence rate: the initial movement period (which lasts from when a station begins to subside to when the subsidence rate is greater than 1.67 mm/day), the active movement period (during which the subsidence rate is greater than 1.67 mm/day), and the attenuation period (which lasts from when the subsidence rate is less than 1.67 mm/day to when the subsidence rate is less than 0.167 mm/day) (He et al. 1991).

In this study, Station A27 on the SOC of Longwall 7226 was found to exceed the above three periods (Fig. 8a). The subsidence value of the initial movement period was 50.0 mm (I; Fig. 8a). The active movement period and attenuation period lasted for 154 and 437 days, respectively, and the subsidence values were 2320.0 and 139.2 mm, respectively (II, III; Fig. 8a). Thus, it can be concluded that the subsidence during the active movement period without grouting was very severe, with an average subsidence rate of 15.01 mm/day. However, the subsidence

**Fig. 5** Final horizontal displacement vectors of the monitoring stations



during the attenuation period was much smaller, with an average subsidence rate of 0.32 mm/day, accounting for 5.5 % of the total subsidence, even though the duration was longer.

By contrast, the subsidence value during the initial movement period with grouting (e.g., 50.6 mm for Station B10; I; Fig. 8b) was similar to that without grouting. However, the subsequent subsidence characteristics with grouting—characterized by a remarkable reduction in the duration, subsidence value, and subsidence rate (II; Fig. 8b)—were obviously different from those without grouting. With GIO, the duration of the active movement period and the corresponding subsidence were 86 days and 300.2 mm with reduction ratios of 44.2 and 87.1 %, respectively. Since the surface subsidence during the active movement period causes the most severe damage to ground buildings, these clear reductions with grouting indicate that GIO has control on not only the final subsidence, but also the dynamic process of surface subsidence.

However, an active phenomenon that led to a total subsidence of 146.1 mm in 48 days (III-2; Fig. 8b) was evident during the attenuation period (III; Fig. 8b) before the subsidence was finally attenuated (III-3; Fig. 8b). It is inferred that this phenomenon was due to the early termination (1–2 months earlier than under normal conditions) of GIO, associated with the seepage of slurry into the mine on the day extraction of Longwall 7226 was stopped. Owing to the early termination of grout injection, the subsidence value reached 397.7 mm over the entire attenuation period (III; Fig. 8b), unexpectedly accounting for 53.1 % of the total subsidence, which is 9.7 times that under traditional longwall extraction without grouting. It was deduced that if GIO was implemented well, the active phenomenon (III-2; Fig. 8b) would not have occurred, and the final amount of subsidence control would have been greater. Therefore, GIO should continue for 1–2 months after the extraction of the working face is complete.

**Fig. 6** Final deformations of measurement line A without grouting (a) and line B with grouting (b). A31–A30 symbolizes the inclination and horizontal strain of the midpoint between Station A31 and Station A30. A30' symbolizes the curvature of the midpoint between A31–A30 and A30–A29. The rest are defined in the same manner

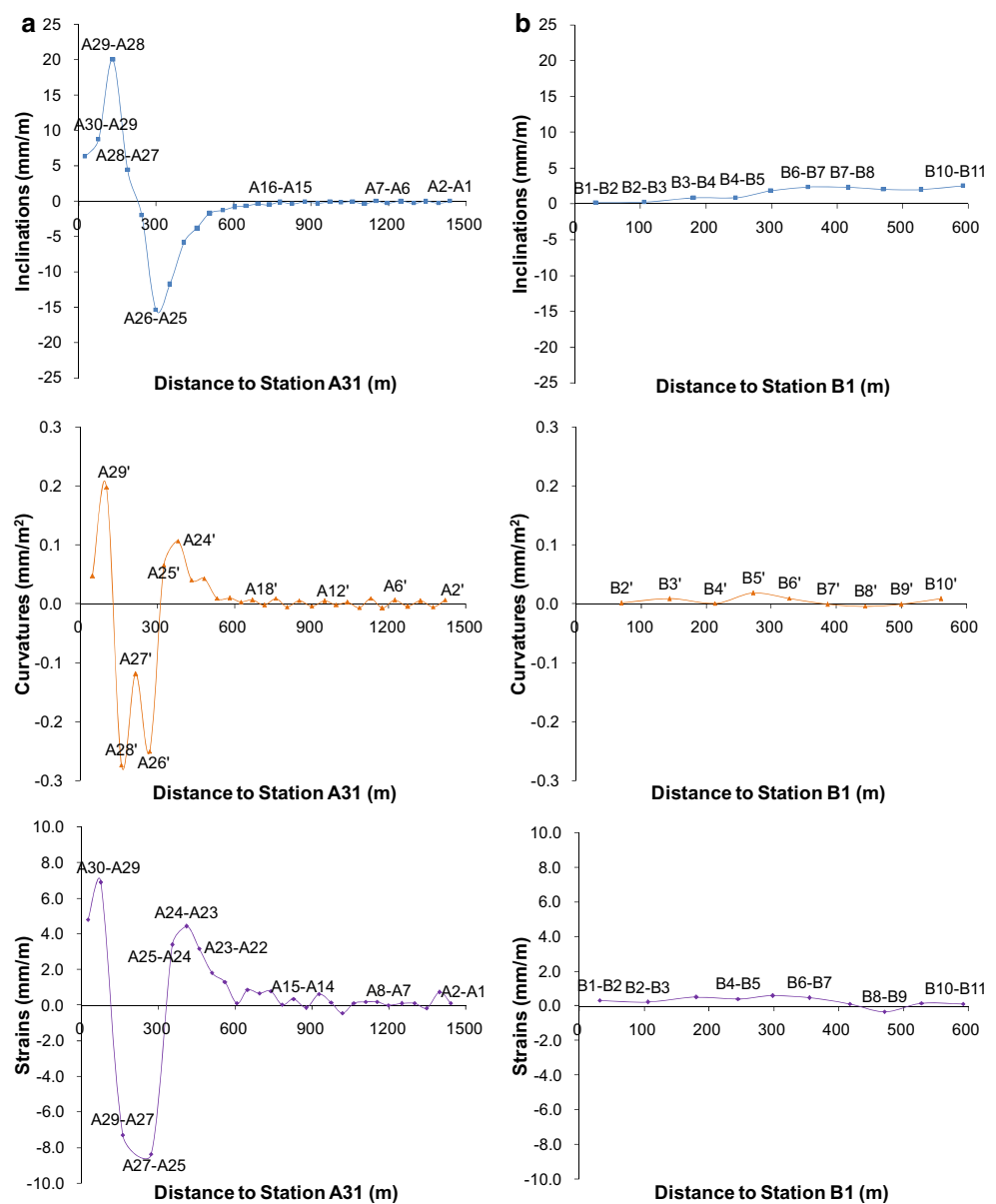


**Table 2** Maximum deformations of measurement line A without grouting and line B with grouting

Deformations	Without grouting		With grouting		Reduction ratio (%)
	Station	Value	Station	Value	
Inclinations (mm/m)	A29–A28	20.04	B6–B7	2.35	88.3
Curvatures (mm/m <sup>2</sup> )	A28'	−0.27	B5'	0.02	92.6
Strains (mm/m)	A27–A25	−8.37	B5–B6	0.59	93.0

It should be noted that the above surface subsidence characteristics associated with GIO are based on the particular case of GIO being implemented on the SSL of a longwall. These characteristics differ from those when GIO is implemented on an entire longwall, as in the cases by

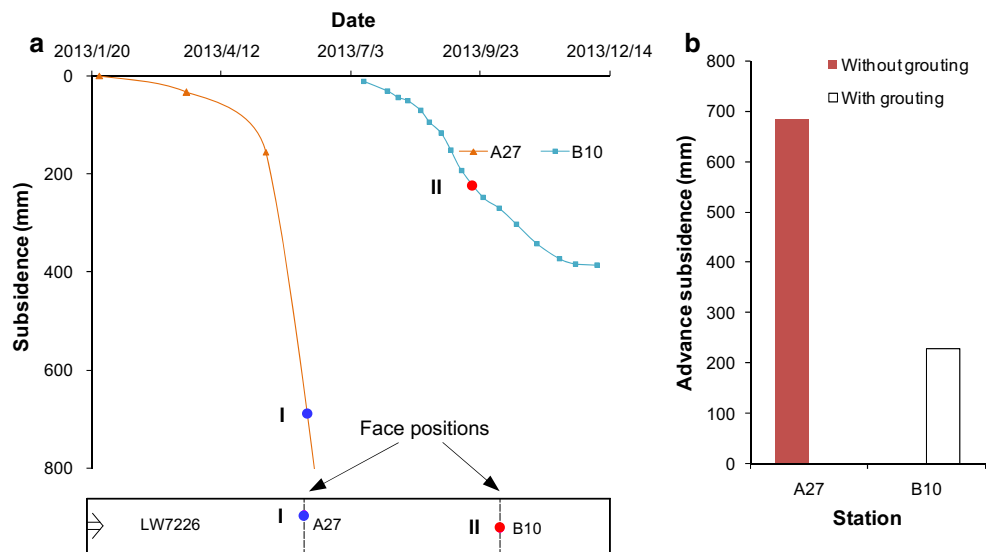
Xuan and Xu (2014). When GIO on the SSL of Longwall 7226 began, the SOC had already been extracted without grouting, which disturbed the surface and subsurface of the SSL. Thus, a better control of subsidence would be expected if GIO were implemented on an entire longwall,



**Table 3** Classification of damage to surface brick–concrete constructions (State Bureau of Coal Industry 2000)

Damage level	Surface deformations			Classification	Structural processing
	Strains (mm/m)	Curvatures (mm/m <sup>2</sup> )	Inclinations (mm/m)		
I	≤2.0	≤0.2	≤3.0	Negligible damage	No repair
				Very slight damage	Light repair
II	≤4.0	≤0.4	≤6.0	Slight damage	Minor repair
III	≤6.0	≤0.6	≤10.0	Medium damage	Medium repair
IV	>6.0	>0.6	>10.0	Severe damage	Heavy repair
				Very severe damage	Demolition and construction

**Fig. 7** Advance subsidence of Station A27 without grouting and Station B10 with grouting. **a** Curves for subsidence of Stations A27 and B10 and a diagram of Longwall 7226. “I” and “II” represent surface subsidence when the working face was directly under Stations A27 and B10, respectively. **b** Histogram for advance subsidence of Stations A27 and B10



that is, if grouting injection was started right after the working face advanced at a certain distance. Nevertheless, the control of subsidence on the SSL of Longwall 7226 met the protection standards of the ground buildings, despite the unfavorable conditions. This shows that GIO is an effective method for controlling the surface subsidence in coal mining areas.

**Conclusions**

The subsidence characteristics when GIO is implemented on the SSL of a coalmine longwall were examined in this study through in situ monitoring. In addition, the dynamic process of subsidence with grouting on the SSL and those without grouting on the SOC were compared. The research results confirm that GIO is effective in controlling the final and dynamic subsidence. The reduction ratios of the final maximum vertical displacement, horizontal displacement, and subsidence rate were 70.2, 80.4, and 77.5 %,

respectively. These results indicate that the ground buildings were protected well. However, 4.6 % of the mining height subsided at a certain surface point on the SSL before GIO controlled subsidence at that point. Thus, it is considered that the greater the mining height, the more difficult it is to protect the buildings. With grouting, the duration of the active movement period was reduced by 44.2 % and the corresponding subsidence was reduced by 87.1 %, as compared to cases when no grouting is implemented. The study results also show that if GIO is terminated too early after the extraction of the working face is complete, an active phenomenon may occur during the attenuation period. Therefore, to achieve greater control of surface subsidence, grout injection should be continued for 1–2 months after the working face stops advancing.

It should be noted that the above surface subsidence characteristics of GIO were obtained through examination of grouting on the SSL of a longwall. Generally, it is more difficult to protect the ground buildings when GIO is implemented on the SSL than on an entire longwall. In

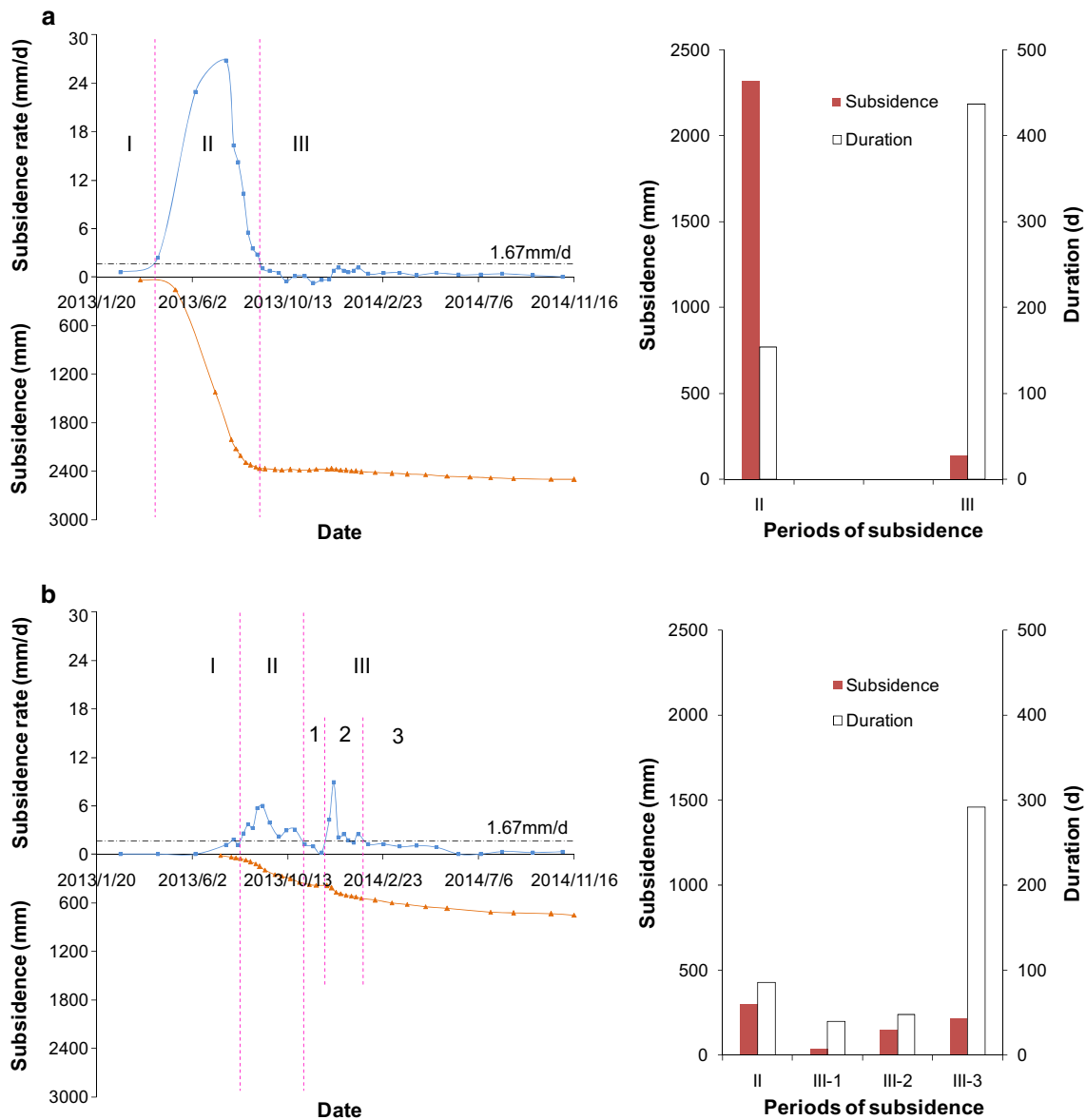


**Fig. 8** Duration of surface subsidence of Station A27 without grouting and Station B10 with grouting. **a** Curves for subsidence and subsidence rate of Station A27 without grouting and histogram for subsidence and duration during the active movement period (II) and attenuation period (III). **b** Curves for subsidence and subsidence

rate of Station B10 with grouting and histogram for subsidence and duration during the active movement period (II) and attenuation period (III). II-2 represents the active phenomenon associated with the early termination of GIO

other words, if GIO is used on an entire panel, a greater control of subsidence will be obtained. Therefore, the success of GIO on the SSL of Longwall 7226 under unfavorable conditions demonstrates that GIO is effective in controlling the surface subsidence in coal mining areas.

**Acknowledgments** This work is supported by “the Fundamental Research Funds for the Central Universities (2014ZDPY28).” The authors are grateful to the Huaibei Mining Group Co., Ltd. for the support during the field tests.

**References**

Can E, Kuşçu Ş, Kartal ME (2012) Effects of mining subsidence on masonry buildings in Zonguldak hard coal region in Turkey. *Environ Earth Sci* 66(8):2503–2518

Can E, Mekik Ç, Kuşçu Ş, Akçın H (2013) Monitoring deformations on engineering structures in Kozlu Hard Coal Basin. *Nat Hazards* 65(3):2311–2330

Chen SG, Guo H (2008) Numerical simulation of bed separation development and grout injecting into separations. *Geotech Geol Eng* 26(4):375–385

- Choi J, Kim K, Lee S, Won J (2010) Application of a fuzzy operator to susceptibility estimations of coal mine subsidence in Taebaek City, Korea. *Environ Earth Sci* 59(5):1009–1022
- de los Cobos G (2015) A historical overview of Geneva's artificial recharge system and its crisis management plans for future usage. *Environ Earth Sci* 73(12):7825–7831
- Dong S, Samsonov S, Yin H, Yao S, Xu C (2015) Spatio-temporal analysis of ground subsidence due to underground coal mining in Huainan coalfield, China. *Environ Earth Sci* 73(9):5523–5534
- Guo H, Shen B, Chen S (2007) Investigation of overburden movement and a grout injection trial for mine subsidence control. In: *Proceedings of 1st Canada/United States rock mechanics symposium, Vancouver*, pp 1559–1566
- He GQ, Yang L, Ling GD, Jia FC, Hong D (1991) *Mining subsidence engineering*. China University of Mining and Technology Press, Xuzhou
- Junker M, Witthaus H (2013) Progress in the research and application of coal mining with stowing. *Int J Min Sci Technol* 23(1):7–12
- Lokhande RD, Prakash A, Singh KB, Singh KKK (2005) Subsidence control measures in coalmines: a review. *J Sci Ind Res India* 5(64):323–332
- Palarski J (1989) The experimental and practical results of applying backfill. In: *Proceedings of the 4th international symposium on mining with backfill, Balkema*, pp 33–37
- Singh KB (2007) Pot-hole subsidence in Son-Mahanadi Master Coal Basin. *Eng Geol* 89(1–2):88–97
- State Bureau of Coal Industry (2000) *Regulations of coal pillar design and extraction for buildings, water bodies, railways, main shafts and roadways*. Coal Industry Press, Beijing
- Witthaus H, Gutberlet K, Junker M (2013) Stowing on longwall faces on the basis of experience acquired in the German coal mining industry. *Min Rep* 149(S1):17–28
- Wu Q, Pang J, Qi S, Li Y, Han C, Liu T, Huang L (2009a) Impacts of coal mining subsidence on the surface landscape in Longkou city, Shandong Province of China. *Environ Earth Sci* 59(4):783–791
- Wu X, Jiang X, Chen Y, Tian H, Xu N (2009b) The influences of mining subsidence on the ecological environment and public infrastructure: a case study at the Haolaigou Iron Ore Mine in Baotou, China. *Environ Earth Sci* 59(4):803–810
- Xuan D, Xu J (2014) Grout injection into bed separation to control surface subsidence during longwall mining under villages: case study of Liudian coal mine, China. *Nat Hazards* 73(2):883–906
- Xuan D, Xu J, Zhu W (2013) Backfill mining practice in China coal mines. *J Mines Metals Fuels* 61(7–8):225–234
- Xuan D, Xu J, Zhu W (2014) Dynamic disaster control under a massive igneous sill by grouting from surface boreholes. *Int J Rock Mech Min* 71:176–187
- Xuan D, Xu J, Wang B, Teng H (2015) Borehole investigation of the effectiveness of grout injection technology on coal mine subsidence control. *Rock Mech Rock Eng*. doi:10.1007/s00603-015-0710-5
- Zhang J, Zhang Q, Sun Q, Gao R, Germain D, Abro S (2015) Surface subsidence control theory and application to backfill coal mining technology. *Environ Earth Sci* 74(2):1439–1448